IEEE Access
Multidisciplinary | Rapid Review | Open Access Journal

Received May 17, 2019, accepted June 17, 2019, date of publication June 24, 2019, date of current version July 11, 2019.

Digital Object Identifier 10.1109/ACCESS.2019.2924462

Using a Digital Camera Combined With Fitting Algorithm and T-S Fuzzy Neural Network to Determine the Turbidity in Water

PINGPING CAO[1], WENZHU ZHAO[1], SHENG LIU[1], LI SHI[1,2], AND HONGWEN GAO[3]

[1]College of Computer Science and Technology, Huaibei Normal University, Huaibei 235000, China
[2]School of Management, Hefei University of Technology, Hefei 230009, China
[3]College of Environmental Science and Engineering, Tongji University, Shanghai 200092, China

Corresponding author: Sheng Liu (liurise@139.com)

This work was supported in part by the National Natural Science Foundation of China under Grant 71801108, and in part by the Natural Science Fund for Colleges and Universities of Anhui Province under Grant KJ2017ZD32 and Grant KJ2017A391.

ABSTRACT We developed a method using a digital camera combined with fitting algorithm and T-S fuzzy neural network (T-S fnn) to measure the water turbidity accurately and efficiently. A turbidity-measuring device and image-processing software based on the common camera were designed to obtain the image of a standard solution after a constant light source passed through the sample and the RGB values, Lab values corresponding to the image were obtained. These RGB values were used as the input of the fuzzy neural network prediction model, the corresponding standard turbidity values were used as the output, and a camera-based fuzzy neural network turbidity measurement method was established. Simultaneously, the standard curve of turbidity measurement is established by fitting the turbidity using color component and color difference. The proposed method was applied to the measurement of standard turbidity solution and the results were compared with those of turbidmeter. The accuracy of the fuzzy neural network and the fitting algorithm is higher than that of the turbidimeter, and the accuracy of the fuzzy neural network method is the highest, the measurement error was only $\pm 0.89\%$, and the accuracy much higher than that of an ordinary turbidimeter. By comparing the independent sample t-tests of the actual water samples, the fuzzy neural network method had the same trend as the turbidimeter and there was no significant difference of the results. The water turbidity measurement with the camera-T-S fuzzy neural network assembly can be applied to the actual water samples. This method can replace the traditional photoelectric detection method to measure turbidity, and it can reduce measurement error and cost. It may be used in environmental detection, biomedicine, and other fields.

INDEX TERMS Color component, curve fitting, digital camera, image processing, T-S fnn, turbidity measurement, water quality.

I. INTRODUCTION

Water quality detection plays an important role in pollution control. It is an important basis for the correct judgment and evaluation of water environments and the comprehensive utilization of wastewater [1]. Water turbidity is also an important indicator in determining whether tap water is drinkable. Measuring the turbidity of tap water is essential before the water leaves the factory. The turbidity requirement for drinking water is less than three NTU in China. As a direct indicator of water quality, turbidity is defined as the reduction in the transparency of a liquid sample caused by the presence of undissolved matter [2]. Turbidity is also sometimes defined sedimentologically, as a measure of the fine particulate material that has a relatively long suspension time in the water column, making it both temporally and physically distinct from the relatively rapid settling of coarser sediment. The turbidity measurement plays a crucial role in industrial, medical, and scientific research, for example, water quality assessment, monitoring of watershed conditions [3], cell culturing, and research on nutrients and bacteria [4], [5].

Too high of a turbidity will hinder the photosynthesis of vegetation in water and affect the growth of vegetation [6]. The successful implementation of farmland

The associate editor coordinating the review of this manuscript and approving it for publication was Yong Yang.

irrigation projects is also closely related to the turbidity of water. Excessive turbidity of water will block sprinkler heads and reduce the uniformity coefficient of the effluent, which will affect the irrigation efficiency [7], [8]. In addition, the excessive turbidity affects the reservoirs' water storage capacity [9], [10]. Therefore, water quality management departments need to accurately measure water turbidity in order to control within a reasonable range so as not to affect the ecological balance and human health.

Whipple and Jackson [11] invented the Jackson Candle turbidimeter in 1900. The light from a candle flame is transmitted through water samples, and the intensity of the transmission is compared with a standard suspension of diatomite [12]. At present, all of the turbidity measurement methods are based on the optical methods including visual turbidimetry, a detection method based on the transmitted the scattered light, and a detection method based on the transmission-scattering ratio. The visual turbidimetry method using turbidimeter or spectrophotometer has a low accuracy and is generally used for the rough evaluation of the water turbidity. The measuring principle is shown in Figure 1.

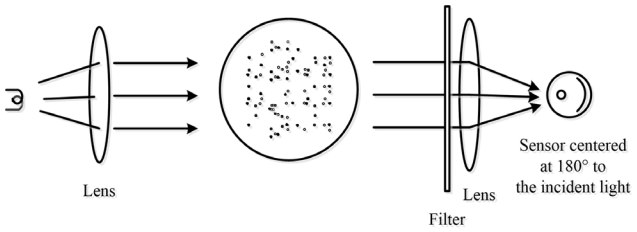

FIGURE 1. Turbidity measurement principle based on transmission.

The relationship between the transmitted light intensity and turbidity is shown in Equation 1.

$$I_T = I_0 e^{(-kdl)} \tag{1}$$

where I_T is the intensity of the transmitted light, I_0 is the intensity of the incident light, k is the proportional constant, d is the solution turbidity, and l is the transmission depth. Generally, the turbidity of an unknown liquid is calculated after the calibration according to the formula. Because the transmission of light in a turbid liquid is complex, an error could occur when using Equation 1. Measuring the turbidity based on the light scattering method using a scattering light turbidimeter is to detect the light that is 90° incident to the source. The measurement principle is shown in Figure 2.

The relationship between the light intensity after scattering and the number and volume of particles per unit volume liquid compliance with Rayleigh formula:

$$I_S = kI_0 nV^2/\lambda^4 \tag{2}$$

where I_S is the light intensity of scattering, k is the proportional constant, I_0 is the incident light intensity, n is the number of particles per unit volume in the sample, V is the volume of particles in the sample, and λ is the incident

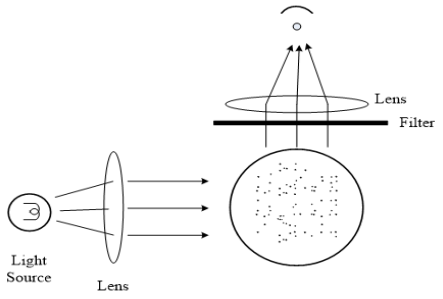

FIGURE 2. Turbidity measurement principle based on light scattering.

light wavelength. However, the scattering turbidimeter usually calculates the turbidity of water using linearity, and so it is suitable only for low turbidity measurements. For a high turbidity, the scattering in the optical path is very complex, and there are multiple times to scatter. It is impossible to accurately determine the relationship between the turbidity and light intensity. Thus, it increases the difficulty of making an accurate turbidity measurement [12]. When a turbidity of more than 10,000 NTU is measured with a commercial turbidimeter, even professional turbidity instruments have an uncertainty as high as ±10% [13]. The measurement error of an ordinary turbidimeter can be up to $\pm 5\% - \pm 10\%$ in the range of 0-1000 NTU. Recent studies on the turbidity measurement methods include COTS sensors [14]–[16], airborne lidar sounding technology [17], and a sensor design using the nephelometric method [18]. Several on-line monitoring systems for the water quality of domestic tap water, lakes, and rivers based on the Wireless Sensor Network (WSN) were implemented using COTS sensors. These wireless sensor network systems have low power consumption but a high cost, and they depend heavily on the sensors and instruments implemented in the platform. The airborne lidar sounding technology has a high accuracy and practicability, but its cost is high and its calibration work is complex. Sensor design using the nephelometric method is reliable in water quality detection. However, it is uncertain whether this method can measure the turbidity above 100 NTU.

To reduce the measurement error of the turbidity, solve the non-linear problem of the solution turbidity and light intensity after transmission or scattering. We improved the accuracy of the turbidity measurement and increased the measurement range. We developed a novel method for measuring the water turbidity with a digital camera combined with fitting algorithm and T-S fuzzy neural network. The digital camera was used to acquire image information with color and brightness, replacing complex photoelectric detection devices. The T-S fuzzy neural network was used to replace the measurement algorithm to achieve high-precision turbidity measurements.

The T-S fuzzy neural network is a kind of neural network with a strong adaptive ability, which can constantly modify the membership function of the fuzzy subset, make the network converge quickly, and establish a non-linear data

relationship model. It is suitable for small data sets. Fuzzy neural networks are in wide use. The current applications mainly focus on the fields of fuzzy regression, fuzzy control, fuzzy expert system, fuzzy matrix equation, fuzzy modeling, and fuzzy pattern recognition. In this work, an ordinary camera and fuzzy neural network were applied to water quality detection, which broadens the application field of fuzzy neural networks. The new, accurate, economical, and convenient turbidity measurement method can provide a reliable selection for the measurement of water turbidity.

II. INSTRUMENT DESIGN

A. STRUCTURE OF INSTRUMENT SYSTEM

The data set used in this research was acquired by self-made image acquisition equipment and turbidity image processing software. The structure of the system is shown in Figure 3.

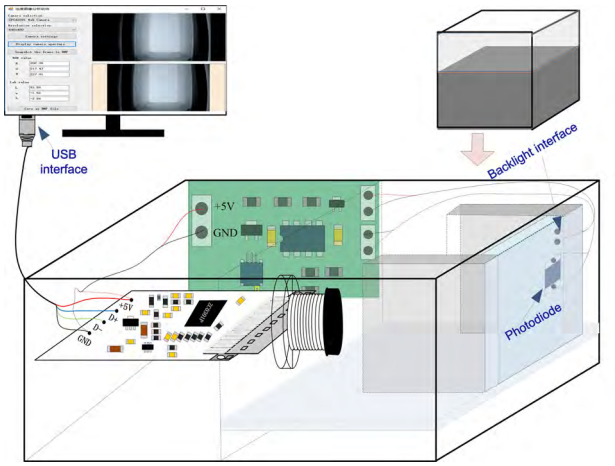

FIGURE 3. Structure diagram of the turbidity image acquisition device.

The device consists of a constant light source circuit, a backlight plate, a sample slot and a digital camera. The shading box seals the sampling area and isolates the external light source, thus avoiding the influence of the external light source on the sampling. The backlight plate is used in the light source system so that the light is uniform; the light source is driven by a constant light source circuit. The backlight plate is closely attached to the colorimetric dish, and the light source consists of 2 0.3 W white LEDs with a color temperature of 5700. When the white light emitted by the backlight plate passes through the turbidity liquid, it absorbs light of a specific wavelength. The turbidity of the liquid is different, and the quality of the substance that absorbs light is different. The absorption of the light is reflected in the image by the camera as soon as the light passes through the liquid.

B. BACKLIGHT CIRCUIT

The light produces images via the digital camera through the liquid being measured. The light source produced by the backlight plate was uniform and the imaging quality was good. The backlight plate is shown in Figure 4a and the circuit in Figure 4c. The circuit is powered by USB. The photodiode

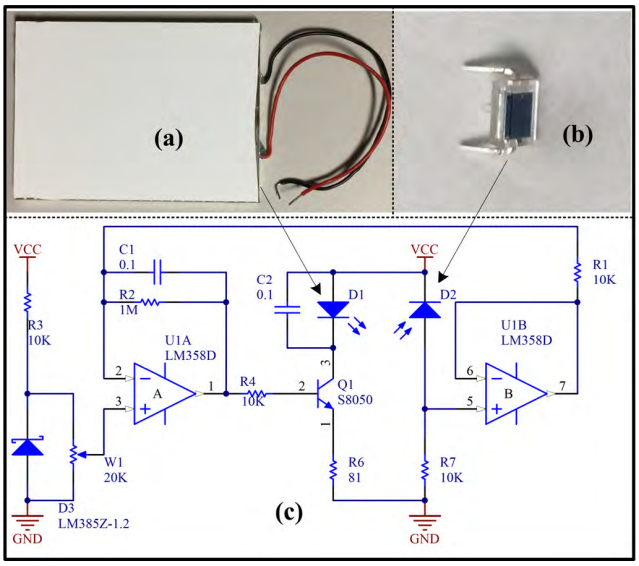

FIGURE 4. Constant light intensity circuit: (a) backlight panel, (b) photodiode, and (c) constant light intensity circuit.

D2 (Figure 4b) collects the light intensity of the backlight plate and generates a voltage signal to control the working current of the backlight plate. Thus this closed-loop control circuit can provide for a constant light intensity.

C. THE DIGITAL CAMERA

The digital camera used in this study was a common camera, but we needed to disable the automatic exposure, brightness, and white balance adjustment functions to ensure the consistency of the parameters throughout the whole measurement process. The camera used in this study was a JD300, and its structure is shown in Figure 5.

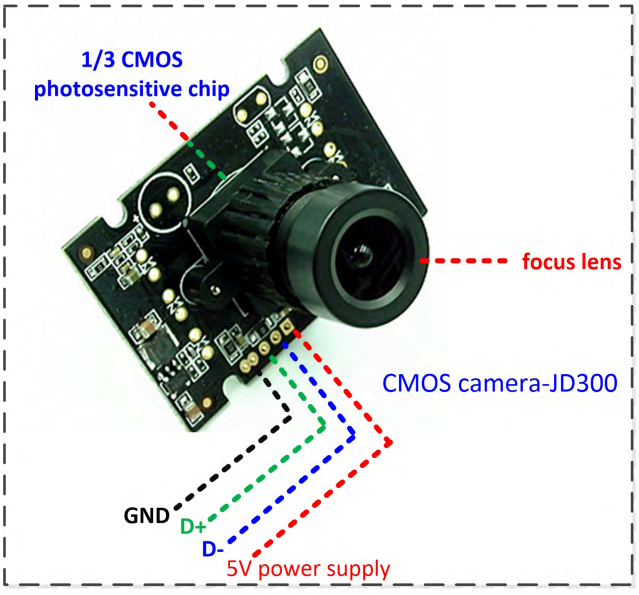

FIGURE 5. Camera PCB details.

D. SOFTWARE DESIGN

The designed software was based on the open source camera tool development kit and C# language. The main function of the software is to obtain the RGB value of the camera image and set the parameters of the camera.

The main interface of the software is shown in Figure 6. A frame image is acquired by the snapshot button. The RGB values of 400 pixels in the central region of the image are read, and then the average RGB values of these pixels are obtained. The camera settings button is used to set up the camera parameters, including the brightness, contrast, hue, saturation, white balance and exposure. These parameters must be fixed to ensure the accuracy of each measurement.

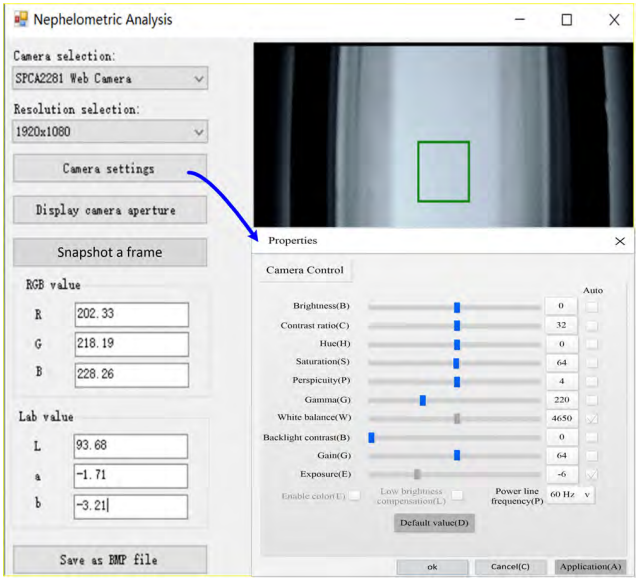

FIGURE 6. Turbidity image analysis software interface.

The data set of the T-S fuzzy neural network water turbidity prediction model is obtained using the RGB value of the turbidity image collected by the software system as the input data and the corresponding turbidity value as the label.

III. METHODS

A. PREPARATION OF STANDARD SOLUTION

The data sets were the RGB values of the 0-1000 NTU standard turbidity liquid images configured by the standard 200, 400, and 1000 NTU turbidity solutions and distilled water. The standard turbidity of liquid is calculated using Equation 3.

$$c = \frac{c_1 l_1 + c_2 l_2}{l_1 + l_2} \tag{3}$$

where c_1 and c_2 are standard turbidity solutions of a known concentration, and l_1 and l_2 are the corresponding solution volumes of c_1 andc_2.

B. CONVERSION FROM RGB COLOR SPACE TO LAB COLOR SPACE

After obtaining the image of turbidity liquid by digital camera, the average RGB value of 400 pixels in the central region of the image is firstly obtained, then the RGB color space is converted to the XYZ color space through color space conversion, and then the corresponding Lab value of the turbidity solution is obtained from the XYZ color space to the Lab color space. The conversion algorithm is as follows:

First, RGB values were converted to XYZ values at:

$$\begin{bmatrix} X \\ Y \\ Z \end{bmatrix} = \begin{bmatrix} 0.412453 & 0.3575800 & 0.180423 \\ 0.213671 & 0.715160 & 0.072169 \\ 0.019334 & 0.119193 & 0.950227 \end{bmatrix} \begin{bmatrix} R \\ G \\ B \end{bmatrix} \tag{4}$$

$$\begin{cases} X = \dfrac{X}{255 \times 0.950456} \\ Y = \dfrac{Y}{255} \\ Z = \dfrac{Z}{255 \times 1.088754} \end{cases} \tag{5}$$

Then, the XYZ values were converted to Lab values:

$$\begin{cases} L = 116 f(\dfrac{Y}{100.0}) - 16 \\ a = 500 \left[f(\dfrac{X}{95.047}) - f(\dfrac{Y}{100.0}) \right] \\ b = 500 \left[f(\dfrac{Y}{100.0}) - f(\dfrac{Z}{108.883}) \right] \end{cases} \tag{6}$$

$$f(t) = \begin{cases} t^{\frac{1}{3}} & if\ t > \left(\dfrac{6}{23}\right)^3 \\ \dfrac{1}{3}(\dfrac{29}{6})^2 t + \dfrac{4}{29} & otherwise \end{cases} \tag{7}$$

C. FITTING METHOD

Because the turbidity is measured by gray scale method, the relationship between R, G, B values and turbidity is close. The turbidity is fitted by R, G, B, L, RGBĄCRGB chromatic and Lab chromatic aberration respectively, and the relationship between various color components and chromatic aberration and turbidity is obtained. The results are compared with those of the T-S fuzzy neural network method.

D. METHOD OF T-S FUZZY NEURAL NETWORK

1) T-S FUZZY NEURAL NETWORK PREDICTION MODEL

The T-S fuzzy system is a kind of self-adaptive fuzzy system. The model can update automatically, as well as modify the membership function of the fuzzy subset. The fuzzy neural network was established according to the principles of fuzzy systems. Each node in the network and its parameters has certain physical meanings. When the network is initialized, the initial values of these parameters can be determined according to the fuzzy or qualitative knowledge of the system. The network can converge quickly and is very suitable for dealing with small data sets (such as the 213 sets of data used in this study).

2) T-S FUZZY NEURAL NETWORK STRUCTURE

The T-S fuzzy neural network is composed of the forward network and the consequent network [19], [21]. Figure 7 shows the structure of the T-S fuzzy neural network.

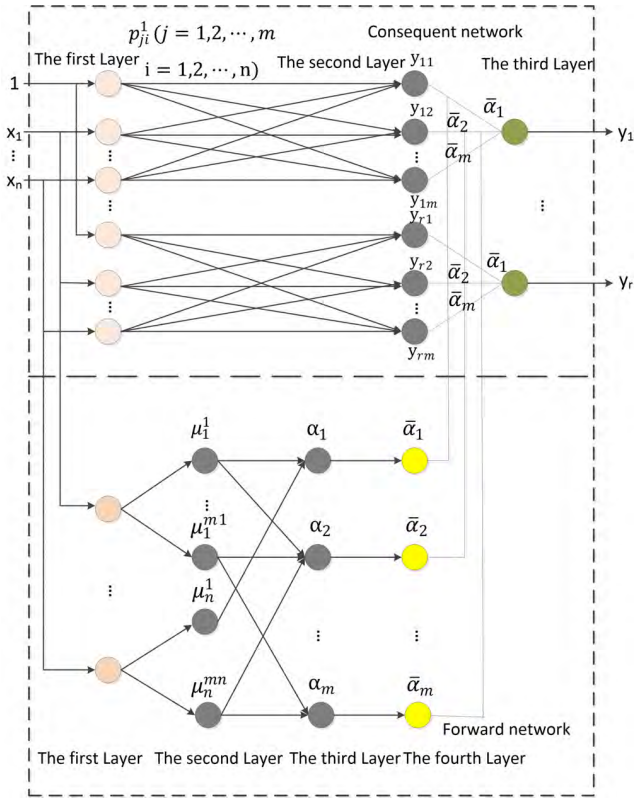

FIGURE 7. Structure of the T-S fuzzy neural network.

The forward network consists of four layers, and the first layer is the input layer. Each node of the input vector is connected directly to the componentx_i of the input vector, and the input value $x = [x_1, x_2, \cdots, x_n]$ is transmitted to the next layer, where the number of nodes $N_1 = n$.

Each node in the second layer represents a linguistic variable value, and the number of nodes in this layer is N_2.

$$N_2 = \sum_{i=1}^{n} m_i \tag{8}$$

For the input $x = [x_1, x_2, \cdots, x_n]$, the membership degree μ_A^i of each input variable x_j is calculated according to the fuzzy membership function.

Fuzzy membership function is a function used to quantitatively calculate the membership of elements. The determination methods of membership function are divided into fuzzy statistics method, assignment method, expert experience method, binary comparative ranking method and borrowing the existing "objective" method. The selection of membership function of T-S fuzzy neural network in this paper is based on the characteristics of our data set and the purpose of prediction. It is preliminarily determined by assignment method and verified by comparison. This design is based on the RGB value of turbidity image to measure water turbidity. The RGB value of turbidity image has an exponential relationship with turbidity. And the expression is: $Y(x) = A^* \exp\left(\frac{tx}{B}\right) + C$ (shown in Figure 10), where A, B, C and t are constant, similar to the expression of Gauss function. Therefore, we inferred that the elements of RGB set can be represented by a Gaussian function, and that the Gaussian function can represent the "true degree" of the elements belonging to the fuzzy set. In addition, the purpose of using T-S fuzzy neural network is to measure water turbidity accurately, which requires higher resolution and measurement accuracy. The fuzzy subset with sharp shape of membership function curve has higher resolution and measurement accuracy, so Gauss function was chosen as the membership function of T-S fuzzy neural network to measure water turbidity. the membership degree μ_A^i of each input variable x_j is:

$$\mu_{A_j^i} = \exp\left(-\frac{\left(x_j - c_j^i\right)^2}{b_j^i}\right) \quad j = 1, 2, \cdots, n; \quad i = 1, 2, , \cdots, k \tag{9}$$

In the formula, A_j^i is the fuzzy set of the fuzzy system, c_j^i and b_j^i are the center and width of the membership function, n is the number of input vectors, and k is the number of fuzzy subsets.

Then, the membership degree is used for the fuzzy calculation, and the fuzzy operators are used as continuous multiplication operators.

$$\omega^i = \mu_{A_j^1}(x_1)^* \mu_{A_j^2}(x_2)^* \cdots^* \mu_{A_j^n}(x_n) \tag{10}$$

Finally, according to Equation (9), the membership function μ_i^j of each input component belonging to the fuzzy set of linguistic variables is calculated:

$$\mu_i^j = \mu_{A_j^i}(x_i) \tag{11}$$

In this equation, $i = 1, 2, \cdots, n$ and $j = 1, 2, \cdots, m_i$. n is the number of inputs, and m_i is x_i's fuzzy partition number.

The third layer is used to match the preconditions of the fuzzy rules. Each node represents a fuzzy rule. The fitness of each rule is calculated by Equation (12), and the number of nodes in this layer is $N_3 = m$:

$$\alpha_j = min\left\{\mu_1^{(i_1)}, \mu_2^{(i_2)}, \ldots, \mu_n^{(i_n)}\right\} \text{ or } \alpha_j = \mu_1^{(i_1)}\mu_2^{(i_2)}\ldots\mu_n^{i_n} \tag{12}$$

In this equation, $i_1 \in \{1, 2, \cdots, m_1\}$,$i_2 \in \{1, 2, \ldots, m_2\}$,…, $i_n \in \{1, 2, \ldots, m_n\}$,$j = 1, 2, \ldots, m$.

$$m = \prod_{i=1}^{n} m_i \tag{13}$$

Given a specific input, only the linguistic variables near the input point have large membership values, while the membership of the remaining points may be very small, such as the Gauss membership function, or 0, such as the triangular membership function. When the membership function is lower than 0.05, the membership function can be considered to be close to 0. There are only a few nodes in α_j whose output is not 0, and most nodes whose output is 0, which is similar to local approximation networks.

The fourth layer carries out the normalization calculation (Equation (14)), and the number of nodes in this layer $N_4 = N_3 = m$.

$$\overline{\alpha}_j = \frac{\alpha_j}{\sum_{i=1}^{m} \alpha_i} (j = 1, 2, \cdots, m) \tag{14}$$

The consequent network consists of r sub-networks with the same structure and each sub-network generates one output. The first layer sub-network is the input layer, which transmits the input variables to the second layer.

The second layer sub-network is used to calculate the consequence of each rule; there are m nodes in this layer, and each node represents a rule, that is,

$$y_{ij} = p^i_{j0} + p^i_{j1} x_1 + \cdots + p^i_{jn} x_n \tag{15}$$

where p^i_j is a parameter of the fuzzy system, $j = 1, 2, \cdots, m$ and $i = 1, 2, \cdots, r$.

The third layer subnetwork is used to calculate the output of the system:y_i.

$$y_i = \sum_{j=1}^{m} \overline{\alpha_j y_{ij}} i = (1, 2, \cdots, r) \tag{16}$$

3) LEARNING ALGORITHMS OF FUZZY NEURAL NETWORKS

Error calculation:

$$e = \frac{1}{2} (y_d - y_c)^2 \tag{17}$$

where y_d is the expected output of the network, y_c is the actual output of the network, and e is the error of the expected output and the actual output.

Coefficient correction:

$$p^i_j(n) = p^i_j(n-1) - \alpha \frac{\partial e}{\partial p^i_j} \tag{18}$$

$$\frac{\partial e}{\partial p^i_j} = (y_d - y_c)\, \omega^i / \sum_{i=1}^{m} \omega^i \cdot x_j \tag{19}$$

where p^i_j is the coefficient of the neural network, α is the learning rate of the network, x_i is the input parameter of the network, and ω_i is the continuous product of the membership degree of the input parameter.

Parameter correction:

$$c^i_j(n) = c^i_j(n-1) - \alpha \frac{\partial e}{\partial c^i_j} \tag{20}$$

$$b^i_j(n) = b^i_j(n-1) - \alpha \frac{\partial e}{\partial b^i_j} \tag{21}$$

4) ESTABLISHMENT OF WATER TURBIDITY PREDICTION MODEL BASED ON THE T-S FUZZY NEURAL NETWORK

The fuzzy neural network determines the number of input and output nodes according to the input and output dimensions of the training samples. In this study, the input data dimension was 3 and the output data dimension was 1, so 3 input nodes and 1 output node were utilized. By analyzing the number of input and output nodes and combining the training and testing results of multiple prediction models when 10 membership functions are selected, the training and testing errors of the prediction model are the lowest, and the results are relatively stable. This approach results in a water turbidity prediction model based on a fuzzy neural network with 3 input nodes, 10 fuzzy nodes, and 1 fuzzy output node. The prediction error of the model is 0.1, the learning rate is 0.05, and the maximum number of training is 1000. The RGB value of the turbidity solution image is used as the input of the model, and the turbidity of a standard turbidity solution is used as the output to train and test the prediction model of the fuzzy neural network. The best parameters and coefficients are calculated by using the fuzzy rules of the fuzzy layer. (We saved these values for the prediction of the actual water samples.) The flow chart of the water turbidity prediction algorithm based on the T-S fuzzy neural network is shown in Figure 8.

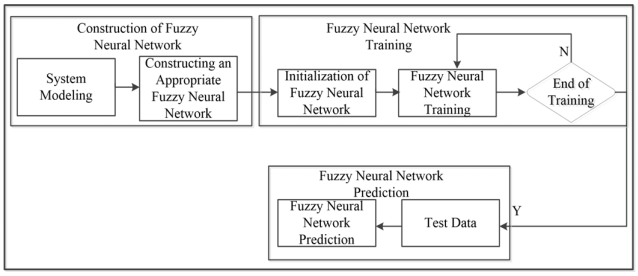

FIGURE 8. Flow chart of the T-S fuzzy neural network algorithm for predicting the water turbidity.

IV. RESULTS AND DISCUSSION

A. ANALYSIS OF TURBIDITY IMAGE

The solution image was obtained using the designed measuring device, and the experimental data were obtained with the software. The partial experimental data obtained are shown in Figure 9.

0 NTU	40 NTU	90 NTU	100 NTU	200 NTU	400 NTU	800 NTU	1000 NTU
R 202.37	R 190.14	R 179.90	R 178.68	R 155.28	R 116.44	R 69.43	R 47.42
G 216.95	G 204.14	G 191.45	G 190.02	G 163.55	G 126.97	G 75.75	G 52.38
B 227.66	B 215.14	B 198.47	B 197.02	B 167.01	B 126.41	B 77.26	B 53.35
L 93.52	L 91.32	L 89.07	L 88.81	L 83.53	L 75.39	L 60.98	L 52.01
a -1.45	a -1.38	a -1.38	a -1.35	a -1.41	a -2.54	a -1.82	a -1.88
b -3.29	b -3.46	b -2.57	b -2.47	b -1.60	b -0.67	b -1.43	b -1.31

FIGURE 9. Partial standard turbidity solution image.

With the increase of the turbidity, the brightness of the turbidity image decreases gradually, and the RGB value also changes. The variation of the RGB and Lab values of the turbidity images is shown in Figure 9.

B. FITTING RESULTS OF TURBIDITY TO COLOR COMPONENT OR COLOR DIFFERENCE

In addition to the RGB data of image, the software acquired the Lab value to track the change of the solution's brightness.

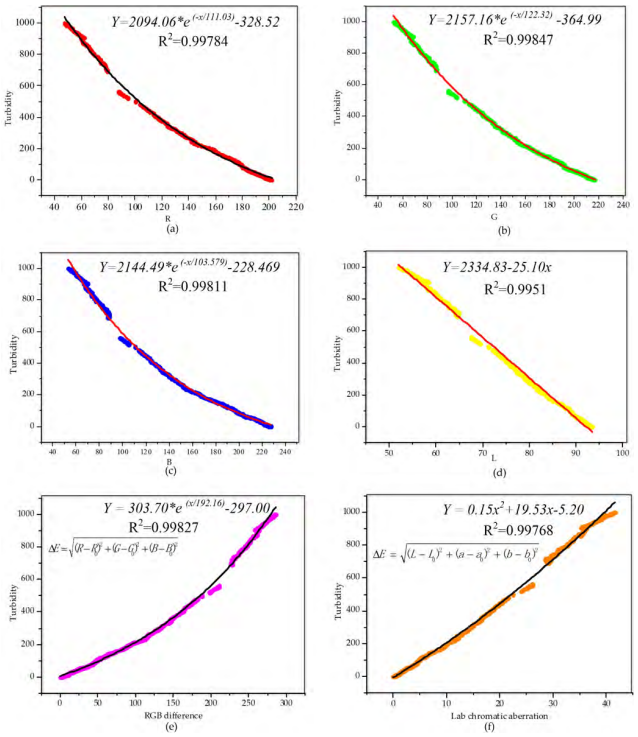

FIGURE 10. Standard curve of color component to turbidity.

The RGB and Lab values can be used to establish the relationship to turbidity. The standard curves are shown in Figure 10.

The fitting curves between RGB and turbidity are shown in Figure 10 a, b and c where all of them are non-liner. The Lab value is obtained from the RGB value of the solution image by the color space conversion. Figure 10d shows that the brightness (L) of the solution has a linear relationship with the turbidity. ''a'' denotes the range from red to green, and ''b'' from yellow to blue. Figure 10 e and f are the standard curves, i.e. the RGB color difference and Lab colors' difference V.S. the turbidity. The color difference refers to that between the turbidity solution and the blank solution.

The results are fitted to be shown in Table 1.

TABLE 1. Standard curve expressions.

Fitting Object	Standard Curve	Adj. R^2
R	$Y = 2094.06 * \exp(-x/111.03) - 328.52$	0.99784
G	$Y = 2157.16 * \exp(-x/122.32) - 364.99$	0.99847
B	$Y = 2144.49 * \exp(-x/103.579) - 228.469$	0.99811
L	$Y = 2334.83 - 25.10x$	0.9951
RGB Chromatic Aberration	$Y = 303.70 * \exp(x/192.16) - 297.00$	0.99827
Lab Chromatic Aberration	$Y = 0.15x^2 + 19.53x - 5.20$	0.99768

C. PREDICTION WITH THE T-S FUZZY NEURAL NETWORK PREDICTION MODEL

The RGB values in the training data set were used as the feature input, and the corresponding turbidity values were used as the learning label to input into the T-S fuzzy neural network prediction model. The model was trained 1000 times and the training results are shown in Figure 11.

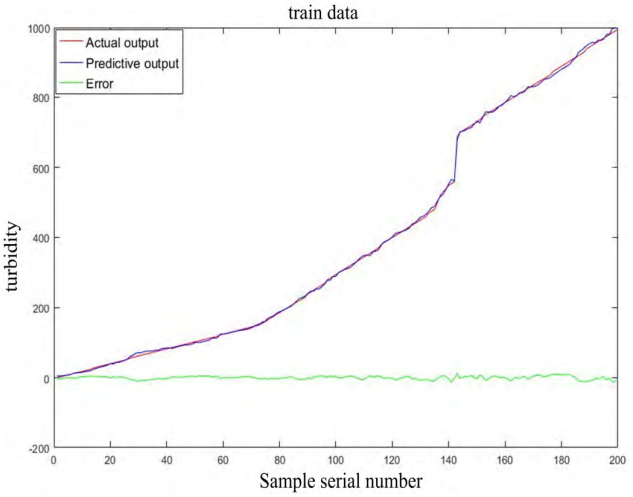

FIGURE 11. Training results of the training data set.

Figure 11 shows that the actual turbidity in the training data is very close to the predicted turbidity. The error fluctuates around 0. The training effect of the model is very good.

The resulting parameters obtained from the repeated training of the training data were applied to the test data for prediction. The stability and accuracy of the prediction model were determined. The predicted results of the test data are shown in Figure 12.

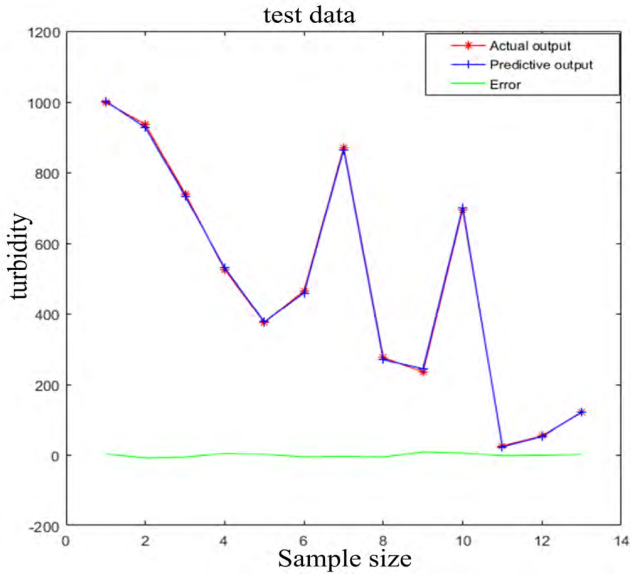

FIGURE 12. Test data set prediction results.

D. THE EFFECT OF DIFFERENT MEMBERSHIP FUNCTIONS ON MEASUREMENT RESULTS

The typical membership functions with sharp curves are triangular, sigmoid and Gauss functions.

TABLE 2. Comparison of predicted results of different functions with standard solutions.

Membership function	Standard solution/NTU						Mean error	Std Dev
Standard solution	935	740	375	275	54	120		
Gauss	926.2645	733.5134	376.6235	268.8904	52.6043	121.5525	3.9839	5.2075
Triangular	936.0819	720.1916	372.2178	274.9097	58.9420	120.6265	4.8885	8.4272
Sigmoid	916.3980	719.6590	367.5880	275.4942	57.7116	120.7556	8.5527	11.7567

1) Triangular membership function:

$$u(x) = \begin{cases} 1 - \dfrac{|x-m|}{\sigma} & |x-m \le \sigma| \\ 0 & \text{other} \end{cases} \tag{22}$$

In the formula, m and σ are the center and width of the fuzzy set.

2) Sigmoid membership function:

$$\mu(x) = 1/(1 + \exp[-a(x-c)]) \tag{23}$$

In the formula,c and a are the center and width of the fuzzy set.

3) Gauss membership function:

$$\mu\,(x) = \exp\left[-\frac{(x-c)^2}{\sigma^2}\right] \tag{24}$$

In the formula,c and σ are the center and width of the fuzzy set.

In order to verify the rationality of selecting the Gauss function as the membership function according to the characteristics of the data set, it also reflects the importance of selecting the membership function correctly. Triangle, Sigmoid and Gauss function are selected to predict water turbidity of T-S fuzzy neural network. The above three functions are respectively applied to T-S fuzzy neural network to predict the standard solution. Some of the predicted results are shown in the Figure 13.

The predicted results of the three functions are compared with the turbidity values of standard solutions, some of which are shown in Table 2.

The comparison results of Figure 13 and Table 2 show that the accuracy of T-S fuzzy neural network using Gauss function to measure water turbidity is higher than that of Triangle and Sigmoid function. The results show that the measurement accuracy is higher when the trend of the fuzzy data set is close to the membership function, and the importance of the selection of membership functions to the measurement results was also verified.

E. COMPARISON WITH STANDARD SOLUTION

ISO (7027-1:2016) specifies two quantitative methods of using optical turbidimeters or nephelometers for the determination of turbidity of water [22]. The turbidimeter used in comparative experiments in this paper is designed according to ISO (7027-1:2016) standard method with the measurement range between 0 to 1000 NTU.

A comparative experiment for measuring the standard turbidity solution was designed and the measurement results of

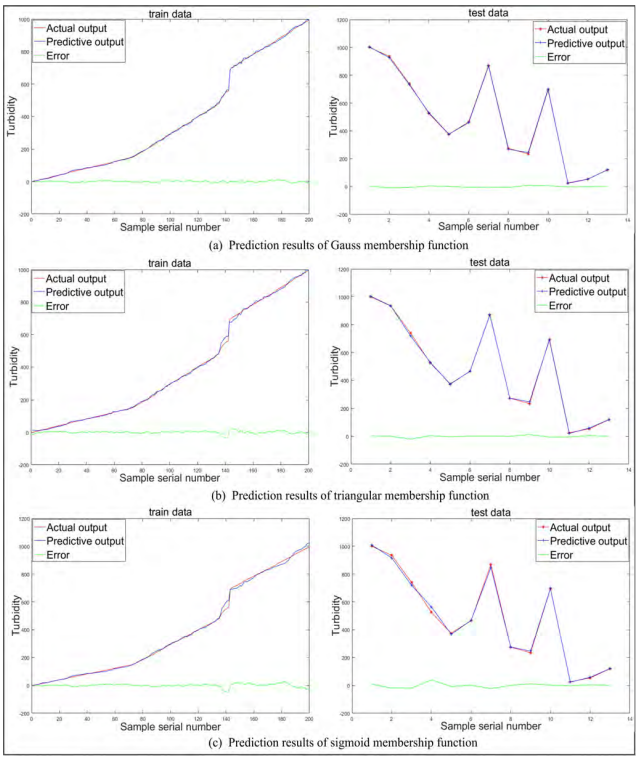

FIGURE 13. Prediction results of different membership functions.

the proposed method were compared with those determined with a Model WGZ-2000 turbidimeter (Shanghai Youke Instruments Company Ltd.). The standard turbidity solution in the test data is determined with the turbidimeter and image method. The partial results are shown in Table 3 and Figure14.

The accuracy of the proposed method is higher than that of the turbidimeter. The standard deviation of T-S fuzzy neural network method is the least and the accuracy the highest.

The proposed method had a higher coincidence with the standard turbidity solution than the turbidimeter. The measurement error was also lower than that of the turbidimeter.

The maximum error of the turbidimeter was about ±4% of the measurement range, but that of the proposed method only ±0.89% of the measurement range.

The measurement results of the methods were closer to the turbidity values of the standard solution within the allowable range of error.

F. DETERMINATION OF ACTUAL WATER SAMPLES

To verify the practicability of the recommended method, several typical lakes in the Huaibei area were selected as the

TABLE 3. Partial test result to standard turbidity solution by different methods.

Methods	Standard solution/NTU						Std Dev
Standard solution	935	740	375	54	275	120	
R curve	927.7845	720.3228	376.0818	62.5512	275.1298	106.1659	10.8394
G curve	928.8493	713.4956	371.1803	56.0059	280.9742	116.8005	11.5820
B curve	929.7736	707.6692	377.1898	52.5030	283.6759	112.8125	14.1807
L curve	908.652	714.64385	396.00627	40.5349	301.39892	112.43649	21.2675
RGB curve	928.9977	713.3206	374.8972	56.2626	280.4484	112.3589	11.8393
Lab curve	931.0958	705.8459	376.0308	53.7672	285.3527	114.8711	14.8119
T-S fnn method	926.2645	733.5134	376.6235	52.6043	268.8904	121.5525	5.2075
Turbidimeter	927.9	735.2	404.3	43.7	304.6	160.5	24.3394

TABLE 4. Measurement results of the two methods for actual local water samples.

Serial number	1	2	3	4	5	6	7
Proposed method	8.6116	11.7751	20.1694	8.3370	12.5149	8.2120	11.2547
Turbidimeter	7.6	10.1	18.6	6.7	10.3	6.2	9.3
Error	1.01	1.68	1.57	1.63	2.21	2.01	1.95
Serial number	8	9	10	11	12	13	
Proposed method	10.9388	11.1283	20.6752	13.676	12.5203	9.6038	
Turbidimeter	9.6	8.9	19.7	11.3	10.6	8.4	
Error	1.34	2.23	0.98	2.38	1.92	1.20	

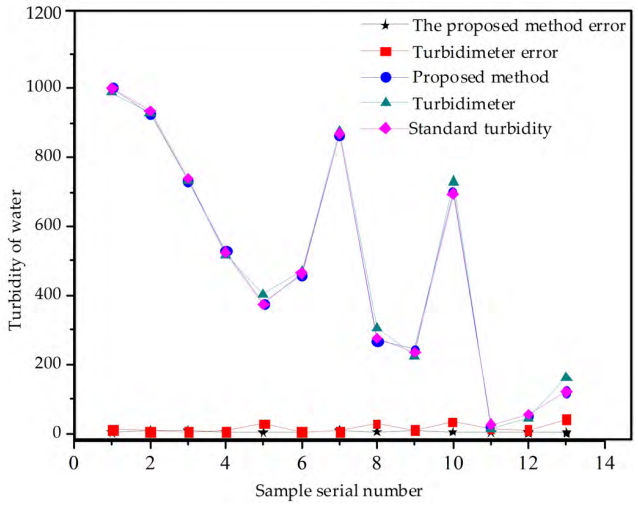

FIGURE 14. Comparison of the results of the turbidimeter with the proposed method.

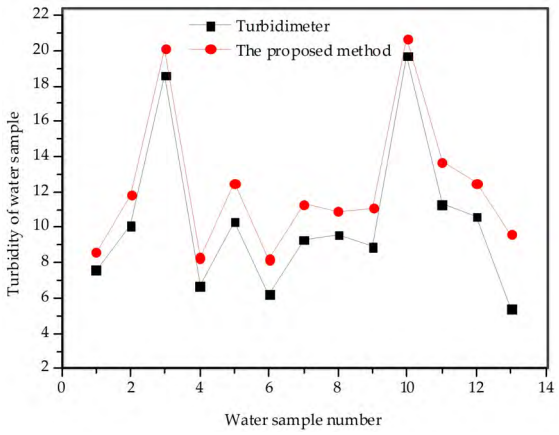

FIGURE 15. Results of the actual water sample measurements using the two approaches.

TABLE 5. Independent sample t-test results of the two methods.

	Turbidity
Proposed method	12.3 ±1.109
Turbidimeter	10.6±1.136
t	1.071
p	0.295

water sampling points. The digital camera combined with the T-S fuzzy neural network and the turbidimeter(Model WGZ-1B, produced by Shanghai Xinrui Instrument Company) were used to evaluate the validation samples. The official error of this turbidimeter was ±5% of the range, and the range was 0-200 NTU. The partial detection results are shown in Table 4.

Table 4 shows that the measurement results(Figure15) between the proposed method and the turbidimeter has a little error.

The independent sample t-test was used for the measurement results of the two methods by SPSS software (Table 5). Table 5 shows the independent sample t-test results for the measurement of the two methods, and the p value is 0.295 (>0.05), which indicates that there is no a significant difference between the two methods. Table 5 and Figure 15 show that the measurement results of the proposed method have

the same trend as those of the turbidimeter. The difference is little, so the proposed method is reliable.

V. ANALYSIS

A. ADVANTAGES OF DIGITAL CAMERA COMBINED WITH IMAGE METHOD

At present, the measurement of turbidity is mainly performed via photoelectric methods, such as spectrophotometry and the instrumental method. Spectrophotometry determines the turbidity by measuring the absorbance at a specific wavelength. The instrumental method determines the turbidity by measuring the scattered light. Both methods use photovoltaic cells or phototubes to convert transmitted or scattered light into electrical signals; the detected analog signal is converted into a digital signal and sent to the MCU for processing. The turbidity value is then displayed.

Digital cameras mostly use the CMOS-photosensitive elements. CMOS-photosensitive elements are semiconductor elements used to record light changes, and they are mainly composed of silicon and germanium. Their advantages are their high integration, low power consumption, and low cost. Each pixel of the camera is equivalent to a photoelectric detection element, and the signal-processing unit integrated by the camera can replace the digital-to-analog conversion circuit and signal-processing circuit of the turbidimeter. Therefore, using a camera and neural network algorithm to measure turbidity avoids the development of a photoelectric detection circuit, signal-processing circuit, digital-to-analog conversion circuit, and display circuit; it can also visualize the turbidity measurement process. The white balance algorithm of the camera can be used for 0 correction, and by adjusting the saturation, the turbidity image can be converted into black-and-white image, and the interference of color on turbidity measurement can be eliminated. The sensitivity of the measurement can be adjusted by adjusting the brightness, contrast, exposure, and light source brightness, which is suitable for turbidity measurements in different ranges. The strong non-linear fitting ability of the neural network can improve the measurement accuracy. Therefore, the application of our image method and neural network for turbidity measurements can achieve the measurement of the turbidity solution accurately, conveniently, and quickly.

B. COMPARING WITH THE LATEST IMAGE METHODS FOR TURBIDITY MEASUREMENT

The latest methods to measure turbidity by image analysis include the following. A turbidity measurement method for natural water based on Hydrocolor was proposed [23], which is based on radiometric measurements instead of image color. It is shown that HydroColor can measure the remote sensing reflectance to within 26% of a precision radiometer and turbidity within 24% of a portable turbidimeter. Compared with our method, this method provided a simple and low cost method for measuring the reflectance and water quality, but the accuracy is low for the HydroColor's ability to measure reflectance and turbidity accurately depend on environmental conditions.

A novel and automatic turbidity estimation system for fluids was proposed [24]. Effluent samples are imaged such that the light absorption characteristic is highlighted as a function of fluid depth and computer vision processing techniques are used to quantify this characteristic. The system has the advantage of easy repetition, and implementing such a system would lead to a reduction in manpower requirements, improve wastewater monitoring frequency. However, when measuring turbidity, the system needs to be calibrated to produce comparable turbidity values, and the accuracy is not guaranteed.

VI. CONCLUSION

A method of measuring water turbidity with a camera combined with fitting algorithm and T-S fuzzy neural network was proposed. Data sets of neural network and data of fitting algorithm were obtained by a self-made measuring device and image-processing software. A prediction model of the water turbidity and standard fitting curve was established to measure the water turbidity. The standard solution and actual water samples were measured and compared with the results of a turbidimeter. Based on the results of the standard solution comparison, the accuracy of our proposed method was much higher than that of an ordinary turbidimeter, and the fuzzy neural network method has the highest accuracy. We compared the results of the camera combined with T-S fuzzy neural network method with the measured results of actual water samples and found they were consistent. The independent sample test of the measurement results was carried out in SPSS, and the practicability and reliability of the design were verified. The method of detecting the water turbidity using a camera combined with the T-S fuzzy neural network has the advantages of high accuracy and process visualization. Our approach can replace the traditional photoelectric detection method and reduce the cost of water turbidity measurements. The proposed method can also replace other methods based on photoelectric detection, and it can be used in environmental detection, biomedicine, and other fields.

REFERENCES

[1] X.-Y. Bao, S. Liu, W.-G. Song, and H.-W. Gao, "Using a PC camera to determine the concentration of nitrite, ammonia nitrogen, sulfide, phosphate, and copper in water," *Anal. Methods*, vol. 10, no. 18, pp. 2096–2101, 2018. doi: 10.1039/C8AY00312B.

[2] H. Liu, P. Yang, H. Song, Y. Guo, S. Zhan, H. Huang, H. Wang, B. Tao, Q. Mu, J. Xu, D. Li, and Y. Chen, "Generalized weighted ratio method for accurate turbidity measurement over a wide range," *Opt. Express*, vol. 23, no. 25, pp. 32703–32717, 2015.

[3] J. R. Gray, G. D. Glysson, J. H. Eychaner, and C. W. Anderson, "Introduction to the proceedings of the federal interagency workshop on turbidity and other sediment surrogates," in *Proc. Federal Interagency Workshop Turbidity Other Sediment Surrogates*, J. R. Gray G. D. Glysson, Eds. Reston, VA, USA: U.S. Geological Surv., 2003, pp. 5–8.

[4] M. A. Uhrich and H. M. Bragg, *Monitoring Instream Turbidity to Estimate Continuous Suspended-Sediment Loads and Yields and Clay-Water Volumes in the Upper North Santiam River Basin, Oregon, 1998–2000*. Reston, VA, USA: U.S. Geological Survey, 2003.

[5] V. G. Christensen, X. Jian, and A. C. Ziegler, *Regression Analysis and Real-Time Water-Quality Monitoring to Estimate Constituent Concentrations, Loads, and Yields in the Little Arkansas River, South-Central Kansas, 1995–99*. Reston, VA, USA: U.S. Geological Survey, 2000.
[6] G. J. Telesnicki and W. M. Goldberg, "Comparison of turbidity measurement by nephelometry and transmissometry and its relevance to water quality standards," *Bull. Mar. Sci.*, vol. 57, no. 2, pp. 540–547, 1995.
[7] P. G. Home and H. N. Ngugi, "A comparative evaluation of Irrigation efficiencies for smallholder irrigation schemes in Murang'a South District," in *Proc. JKUAT Sci., Technol. Industrialization Conf.*, 2012, p. 193.
[8] N. P. Namu and M. J. Raude, "Prediction of water turbidity using artificial neural networks: A case study of kiriku-kiende settling basin in Embu County, Kenya," *Amer. J. Water Resour.*, vol. 5, no. 3, pp. 54–62, 2017.
[9] E. H. Clark, J. A. Havercamp, and W. Chapman, "Eroding soils; The off-farm impacts," *Amer. J. Alternative Agricult.*, vol. 1, no. 2, pp. 95–96, 1985.
[10] F. Reckendorf, "RCA III, sedimentation in irrigation water bodies, reservoirs, canals, and ditches," U.S. Dept. Agricult., Washington, DC, USA, Tech. Rep. NRCS;US201300070366, 1995.
[11] H. F. Muer, "The determination of sulphur in coal by means of Jackson's candle turbidimeter," *Anal. Sci.*, vol. 8, pp. 691–698, 1995.
[12] M. J. Sadar, "Turbidity science," Hach Company, Loveland, CO, USA, Tech. Rep. Tech. Inf. Ser.-Booklet no. 11, 1998.
[13] *2100 Series Laboratory Turbidimeters*, Hach Company, Loveland, CO, USA, Data Sheet LIT2498 Rev 4, 2013.
[14] V. Raut and S. Shelke, "Wireless acquisition system for water quality monitoring," in *Proc. Conf. Adv. Signal Process. (CASP)*, 2016, pp. 371–374.
[15] R. Yue and T. Ying, "A water quality monitoring system based on wireless sensor network & solar power supply," in *Proc. IEEE Int. Conf. Cyber Technol. Automat., Control, Intell. Syst.*, Mar. 2011, pp. 126–129.
[16] F. Adamo, F. Attivissimo, C. G. C. Carducci, and A. M. L. Lanzolla, "A smart sensor network for sea water quality monitoring," *IEEE Sensors J.*, vol. 15, no. 5, pp. 2514–2522, May 2015.
[17] K. Richter and H.-G. Maas, P. Westfeld, and R. Weiß, "An approach to determining turbidity and correcting for signal attenuation in airborne lidar bathymetry," *PFG-J. Photogramm., Remote Sens. Geoinf. Sci.*, vol. 85, no. 1, pp. 31–40, 2017.
[18] A. A. Azman, M. H. F. Rahiman, M. N. Taib, N. H. Sidek, I. A. A. Bakar, and M. F. Ali, "A low cost nephelometric turbidity sensor for continual domestic water quality monitoring system," in *Proc. IEEE Int. Conf. Autom. Control Intell. Syst. (I2CACIS)*, Oct. 2016, pp. 202–207.
[19] J.-Y. Chen, P.-S. Tsai, and C.-C. Wong, "Adaptive design of a fuzzy cerebellar model arithmetic controller neural network," *IEE Proc.-Control Theory Appl.*, vol. 152, no. 2, pp. 133–137, 2005.
[20] L. Xiao, L. Ye, X. Yu-Ru, W. Lei, and Q. Zai-bai, "Fuzzy neural network control of underwater vehicles based on desired state programming," *J. Mar. Sci. Appl.*, vol. 5, no. 3, pp. 1–4, 2006.
[21] B. Jiang, L.-P. Sun, and J. Cao, *Design of T-S Fuzzy Neural Network Controller for Temperature and Humidity in Wood Drying Process*. China: Electric Machines and Control, 2016.
[22] *Determination of Turbidity. Part 1: Quantitative Methods*, Int. Org. Standardization, Geneva, Switzerland, Standard 7027-1, 2016.
[23] T. Leeuw and E. Boss, "The hydrocolor app: Above water measurements of remote sensing reflectance and turbidity using a smartphone camera," *Sensors*, vol. 18, no. 1, p. 256, 2018.
[24] D. Mullins, D. Coburn, L. Hannon, E. Jones, E. Clifford, and M. Glavin, "A novel image processing-based system for turbidity measurement in domestic and industrial wastewater," *Water Sci. Technol.*, vol. 77, no. 5, pp. 1469–1482, 2018.

PINGPING CAO received the B.Eng. degree in electronic engineering technology from Anhui Normal University, Wuhu, China, in 2017. She is currently pursuing the M.Eng. degree in software engineering with Huaibei Normal University. Her research interests are artificial intelligence and artificial intelligence applications. She has participated in the project of breath mass spectrometry and water quality detection. She is currently working on new application technologies of Artificial Intelligence. Her awards and honors include the National Natural Science Foundation of China and received a scholarship from the Huaibei Normal University.

WENZHU ZHAO was born in Huainan, Anhui, China, in 1995. She received the bachelor's degree in computer science and technology from Huaibei Normal University, in 2018, where she is currently pursuing the master's degree in software engineering.

From 2018 to 2019, she studied at Huaibei Normal University and has participated in the National Natural Science Foundation Project. Her research interests include color features and image processing, and the application of instrumentation.

SHENG LIU received the Ph.D. degree in physics from the Graduate University of Chinese Academy of Sciences, in 2012. He is currently a Professor with the School of Computer Science and Technology, Huaibei Normal University, Anhui, China. His current research interests include intelligent instruments, sensor technology, data analysis, and signal processing. In the past few years, he has completed the design of water heavy metal detection instrument, multi-parameter water quality detection instrument, general ionometer, BOD online measurement instrument based on microbial sensor, solid phase extraction instrument, explosive detector based on ion mobility spectrum, and organic mass spectrometry control systems.

LI SHI was born in 1978. She received the B.S. degree in electrical engineering and the automatization specialty, and the Ph.D. degree in management science and engineering from the Hefei University of Technology, Anhui, China, in 2002 and 2012, respectively. Since 2015, she has been an Associate Professor with the School of Computer Science and Technology, Huaibei Normal University. She is currently holds a postdoctoral position with the School of Management, Hefei University of Technology. Her research interests include data analysis and processing.

HONGWEN GAO is currently a Researcher and also a Doctoral Supervisor with Tongji University. His main research fields are water pollution control, environmental chemistry, and environmental detection. He is the academic leader of the Department of Environmental Molecular Sciences, State Key Laboratory of Pollution Control and Resource Utilization, Tongji University.